Decoherence of Flux Qubits due to $1/f$ Flux Noise

F. Yoshihara,[1] K. Harrabi,[2] A. O. Niskanen,[2,3] Y. Nakamura,[1,2,4] and J. S. Tsai[1,2,4]

[1]*The Institute of Physical and Chemical Research (RIKEN), Wako, Saitama 351-0198, Japan*
[2]*CREST-JST, Kawaguchi, Saitama 332-0012, Japan*
[3]*VTT Technical Research Centre of Finland, Sensors, P.O. Box 1000, 02044 VTT, Finland*
[4]*NEC Fundamental and Environmental Research Laboratories, Tsukuba, Ibaraki 305-8501, Japan*

(Received 16 June 2006; published 17 October 2006)

We have investigated decoherence in Josephson-junction flux qubits. Based on the measurements of decoherence at various bias conditions, we discriminate contributions of different noise sources. We present a Gaussian decay function extracted from the echo signal as evidence of dephasing due to $1/f$ flux noise whose spectral density is evaluated to be about $(10^{-6}\Phi_0)^2/\mathrm{Hz}$ at 1 Hz. We also demonstrate that, at an optimal bias condition where the noise sources are well decoupled, the coherence observed in the echo measurement is limited mainly by energy relaxation of the qubit.

DOI: 10.1103/PhysRevLett.97.167001 PACS numbers: 74.50.+r, 03.67.Lx, 85.25.Cp

A Josephson-junction qubit is a macroscopic quantum object realized in superconducting electric circuits [1]. As a solid-state device sitting in the midst of the circuit and on top of the substrate, the qubit inherently interacts with various degrees of freedom which decohere the qubit. For understanding and suppressing the decoherence mechanisms, it is important to identify the dominant noise sources among the many possibilities.

A strategy to tackle this problem is to use the tunability of the qubit. By changing a bias parameter, one can control the qubit energy as well as the coupling between the qubit and a particular degree of freedom in the environment [2]. Therefore, the measurement of the decoherence as a function of the bias parameters provides valuable information about the environmental degrees of freedom. Such a strategy has been applied to charge-phase qubits [3,4], charge qubits [5,6], flux qubits [7], and phase qubits [8,9].

In this Letter, we report a detailed characterization of decoherence in flux qubits based on a similar approach. In a range of bias conditions, we identify flux noise as the dominant source of the qubit dephasing. We observe dephasing due to $1/f$ flux noise which gives rise to a characteristic Gaussian decay function that seems to be hidden in the previous studies by other decoherence mechanisms [4,7]. We also quantify the noise spectrum density. On the other hand, we show that at an optimal bias condition, where those noises are effectively decoupled from the qubit, the echo decay rate [$\sim(3.5\ \mu\mathrm{s})^{-1}$ in one sample] is about a half of the energy-relaxation rate and is limited mainly by the latter process.

The effective Hamiltonian of a flux qubit can be written as $H_0 = -\frac{\varepsilon}{2}\sigma_z - \frac{\Delta}{2}\sigma_x$, where σ_z and σ_x are Pauli matrices [10]. The energy difference between the two eigenstates is given by $E_{01} = \sqrt{\varepsilon^2 + \Delta^2}$. Here Δ is the tunnel splitting between two states with opposite directions of persistent current along the loop, $\varepsilon = 2I_p\Phi_0(n_\phi - n_\phi^*)$ is the energy bias between the two states, and I_p is the persistent current along the qubit loop. We define the normalized magnetic flux in the qubit loop $n_\phi \equiv \Phi_{\mathrm{ex}}/\Phi_0$, using the externally applied flux through the qubit Φ_{ex} and the flux quantum Φ_0. As the flux qubit we study is coupled to a SQUID for readout (Fig. 1), the SQUID bias current I_b also affects flux in the qubit. The normalized I_b-dependent flux is thus defined as $n_\phi^*(I_b) \equiv 0.5 - \Phi_{I_b}/\Phi_0$ so that $n_\phi = n_\phi^*$ corresponds to $\varepsilon = 0$, i.e., degeneracy of the two persistent current states. Note that I_b affects the qubit only through the flux $\Phi_{I_b}(I_b)$ which is induced by the circulating current in the SQUID loop [11].

We characterize the coherence of the qubit through measurements of energy-relaxation, free-induction decay (FID), and echo decay. From those measurements, we

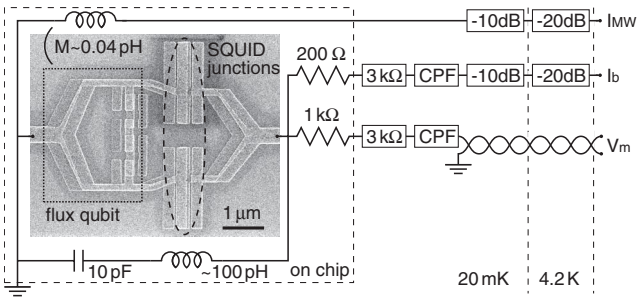

FIG. 1. Scanning electron micrograph of a sample and a sketch of the measurement setup. The qubit shares a part of the loop with a SQUID shunted by an on-chip capacitor. A current bias line (I_b) and a voltage measurement line (V_m) consist of lossy coaxial cables and are connected to the SQUID via on-chip resistors. Microwave current pulses are fed through an on-chip control line (I_{MW}) inductively coupled to the qubit. The sample chip is enclosed in a copper shield box, and all of the wires are electrically shielded as well. CPF stands for a copper-powder filter. Magnetic flux bias is applied with an external superconducting coil connected to a battery-powered current source. The sample is cooled to 20 mK in a dilution refrigerator magnetically shielded with three μ-metal layers at room temperature.

 © 2006 The American Physical Society

deduce the energy-relaxation rate as well as the pure dephasing components in the decoherence. Pure dephasing is caused by the fluctuations of E_{01} which are induced by the fluctuations of parameters λ_i in the Hamiltonian. Here λ_i's could be n_ϕ and I_b as well as other implicit parameters inside Δ and I_p, such as the island charge offsets and the junction critical currents in the qubit. Through the two externally controlled parameters n_ϕ and I_b, we vary the coupling factor $\partial E_{01}/\partial\lambda_i$ and observe the change in the dephasing. Since the derivatives $\partial E_{01}/\partial\lambda_i$ depend differently from each other on the control parameters n_ϕ and I_b, and assuming that the fluctuations of λ_i are independent of the control parameters, we can separate the contributions in the dephasing from different sources.

The experiments were done with samples fabricated by electron-beam lithography and shadow evaporation of Al films (Fig. 1). The qubit is the small superconducting loop intersected by four Josephson junctions [12], among which one is smaller than others by a factor of ~0.56. We have studied five similar samples, and here data from two representative samples are presented. Spectroscopic measurements revealed that I_p and Δ/h were 0.16 μA and 5.445 GHz for sample A, and 0.34 μA and 5.08 GHz for sample B, respectively. The SQUIDs had maximum critical currents of ~3.6 and ~7 μA, and the switching currents under the flux bias used in the qubit readout were ~1.6 and ~4.6 μA, respectively.

The qubit is initialized to the ground state by relaxation and is controlled by a sequence of resonant microwave pulses. The amplitude and the width of the pulses are adjusted so that the desired qubit rotations are implemented. At the end of the pulse sequence, the qubit state is read out by using the SQUID [13]. As the qubit in its eigenstates has a finite expectation value of the persistent current (except for $n_\phi = n_\phi^*$), the critical current of the SQUID is slightly varied corresponding to each eigenstate. Accordingly, the switching probability of the SQUID into the voltage state, responding to a current pulse with a given amplitude and a width, is different for each eigenstate of the qubit [14]. The switching probability $P_{\rm sw}$, which thus reflects the population of the qubit eigenstates, is obtained by repeating the procedure—initialization, control, and readout—a number of times (typically 10^4) and counting the switching events.

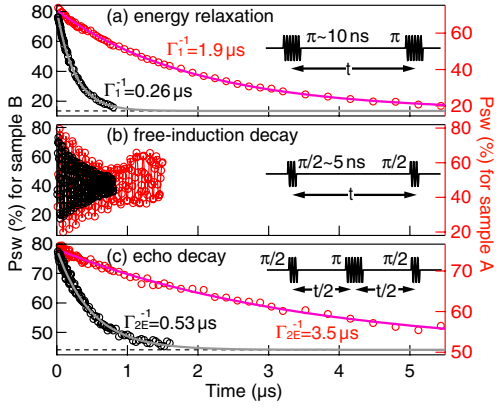

FIG. 2 (color online). Measurements of (a) energy relaxation, (b) free-induction decay, and (c) echo decay at the optimal bias condition $n_\phi = n_\phi^*$ and $I_b = I_b^*$. In each panel, the plot with a longer decay time is for sample A, and the other is for sample B. The insets depict the applied pulse sequence for each measurement. In the measurement of free-induction decay, the microwave carrier frequency was detuned from the qubit frequency E_{01}/h by 10 MHz. Solid curves in (a) and (c) are exponential fits.

Figure 2 shows the results at the optimal bias condition $n_\phi = n_\phi^*$ and $I_b = I_b^*$, where both $\partial E_{01}/\partial n_\phi$ and $\partial n_\phi^*/\partial I_b$ were set to zero so that the dephasing due to fluctuations of n_ϕ and I_b is minimal [7,12]. We find that energy-relaxation and echo signals decay exponentially with rates Γ_1 and Γ_{2E}, respectively, and moreover $\Gamma_{2E} \simeq \Gamma_1/2$. Therefore, at this bias condition the coherence observed in the echo measurement is limited mainly by the energy-relaxation process. In the analysis of $P_{\rm sw}$ as a function of the readout current pulse height (data not shown), we have also found that the qubit relaxes mostly to the ground state, not to the mixture of the ground and excited states. This excludes any classical noise from the possible source inducing the relaxation and suggests that the spontaneous decay of the qubit is the dominant process.

Next we study how the fluctuations of I_b affect the coherence of the qubit. We show that we can discriminate the contribution from that of n_ϕ fluctuations, even though the I_b fluctuations also couple to the qubit through the flux degree of freedom n_ϕ^*. First, we present the result of qubit spectroscopy at various I_b. For each I_b, we swept n_ϕ and

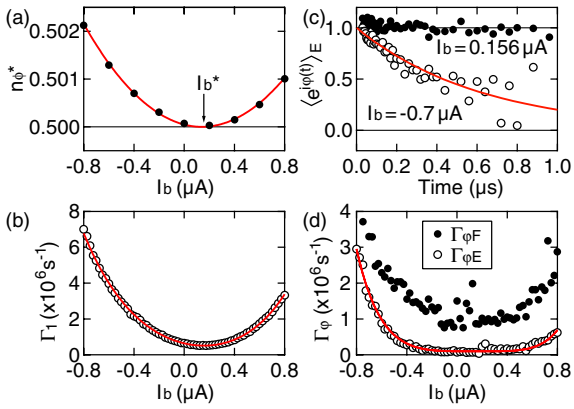

FIG. 3 (color online). Decoherence at various SQUID bias currents I_b (sample A). Qubit flux bias is kept at $n_\phi = n_\phi^*$. (a) Spectroscopically determined n_ϕ^* vs I_b. The solid curve is a polynomial fit. (b) Energy-relaxation rate Γ_1 vs I_b. (c) Dephasing component $\langle e^{i\varphi(t)}\rangle_E$ in the echo measurements for different values of I_b. The solid curve is an exponential decay, $\exp(-\Gamma_{\varphi E}t)$. (d) FID dephasing rate $\Gamma_{\varphi F}$ and echo dephasing rate $\Gamma_{\varphi E}$ as a function of I_b. See text for the explanations of the fitting curves in (b) and (d).

found a minimum of E_{01} to determine n_ϕ^*, which is plotted in Fig. 3(a). Notice that at $n_\phi = n_\phi^*$, $E_{01} = \Delta$ and $\partial E_{01}/\partial n_\phi = 0$. The plot also represents how I_b affects the flux in the qubit and how the fluctuations of I_b are transformed into the fluctuations of n_ϕ^* via $\partial n_\phi^*/\partial I_b$. The interpolated line $n_\phi^*(I_b)$ has a minimum at $I_b^* \equiv 0.156\ \mu$A. At $I_b = I_b^*$, the noise current coming through the SQUID bias line is split symmetrically into two branches of the SQUID and does not produce any fluctuations of the flux in the qubit, i.e., $\partial n_\phi^*/\partial I_b = 0$. The small offset of I_b^* from zero can be attributed to a small asymmetry in the SQUID junction parameters.

We find a few characteristic behaviors in the decay measurements at the bias conditions along the line $n_\phi = n_\phi^*(I_b)$ (Fig. 3). (i) The energy-relaxation and echo decay curves are always exponential for different values of I_b, while the rates Γ_1 and Γ_{2E} largely depend on I_b. (ii) The ratio of pure dephasing rates in the echo measurement ($\Gamma_{\varphi E} \equiv \Gamma_{2E} - \Gamma_1/2$) and the FID measurement ($\Gamma_{\varphi F} \equiv \Gamma_{2F} - \Gamma_1/2$; with Γ_{2F} obtained from exponential fitting of FID envelope [15]), $\Gamma_{\varphi E}/\Gamma_{\varphi F}$, is significantly smaller than 1 at $I_b \approx I_b^*$, while it approaches 1 at larger $|I_b - I_b^*|$. These two facts, the exponential dephasing and the inefficient recovery of the coherence in echo measurement, suggest that the fluctuations introduced by I_b have a relatively uniform spectrum at least up to $\Gamma_{2E}/(2\pi) \sim 10$ MHz. (iii) The I_b-dependent parts of Γ_1 and $\Gamma_{\varphi E}$ are nicely fitted with a term proportional to $(\partial n_\phi^*/\partial I_b)^2$ and $(\partial n_\phi^*/\partial I_b)^4$, respectively. This implies that the I_b-dependent contributions are solely due to I_b fluctuations and that the fluctuations are well decoupled at I_b^*: The Γ_1 can be compared with the expectation from Fermi's golden rule at $n_\phi = n_\phi^*$, i.e., $\Gamma_1 = (\pi/2\hbar^2)(\partial\varepsilon/\partial n_\phi^*)^2 \times (\partial n_\phi^*/\partial I_b)^2 S_{I_b}(E_{01}/\hbar)$ [16]. Therefore, we can estimate the current noise spectrum at the qubit frequency $S_{I_b}[(E_{01}/\hbar) = 2\pi \times 5.445\ \text{GHz}] = 4.4 \times 10^{-27}\ \text{A}^2\text{s/rad}$ corresponding to the zero-point fluctuations of an impedance $\sim 270\Omega$. Also, the fourth power term in $\Gamma_{\varphi E}$ can be understood as a result of the twofold quadratic couplings between E_{01} and n_ϕ^*, and n_ϕ^* and I_b [12,17].

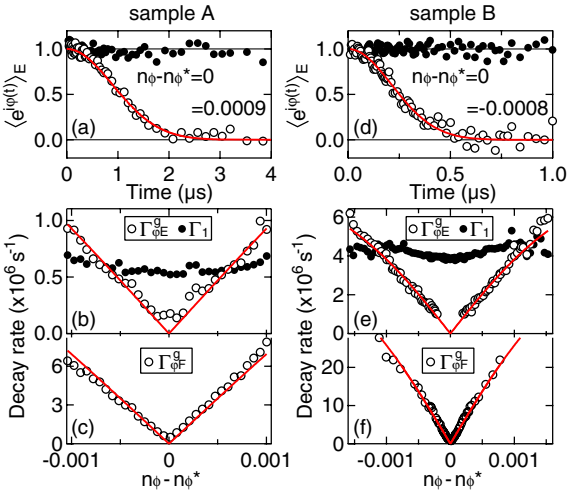

FIG. 4 (color online). Decoherence at various flux biases n_ϕ. SQUID bias current is kept at $I_b = I_b^*$. (a) Dephasing component $\langle e^{i\varphi(t)}\rangle_E$ in the echo measurements for different values of n_ϕ (sample A). The solid curve is a Gaussian fit, $\exp[-(\Gamma_{\varphi E}^g t)^2]$. (b) Energy-relaxation rate Γ_1 and echo dephasing rate $\Gamma_{\varphi E}^g$ vs n_ϕ. The solid line is a $|\partial E_{01}/\partial n_\phi|$ fit to $\Gamma_{\varphi E}^g$. (c) FID dephasing rate $\Gamma_{\varphi F}^g$ vs n_ϕ. The solid line is a $|\partial E_{01}/\partial n_\phi|$ fit. (d)–(f) Data for sample B.

Having seen that the I_b fluctuations can be well decoupled at $I_b = I_b^*$, we now focus on the effect of n_ϕ fluctuations. Compared to the measurements above, measurements at $n_\phi \neq n_\phi^*$ show qualitatively different behaviors (Fig. 4): (i) The energy-relaxation rate Γ_1 is almost constant in the range of n_ϕ, while the dephasing is strongly enhanced as $|n_\phi - n_\phi^*|$ is increased a little. (ii) The echo decay curves are not purely exponential any more, and the extracted dephasing component $\langle e^{i\varphi(t)}\rangle_E$ is fitted with a Gaussian decay, $\exp[-(\Gamma_{\varphi E}^g t)^2]$ [18]. (iii) The decay rate $\Gamma_{\varphi E}^g$ increases almost linearly with $|n_\phi - n_\phi^*|$.

Because of the strong n_ϕ dependence of $\Gamma_{\varphi E}^g$ at around n_ϕ^*, we can rule out possible contributions of charge and critical-current fluctuations in the qubit. Indeed, the observed behaviors are fully consistent with the presence of $1/f$ flux noise. Let us assume Gaussian fluctuations of n_ϕ with the spectrum density $S_{n_\phi}(\omega) = A_{n_\phi}/|\omega|$. Then we calculate $\langle e^{i\varphi(t)}\rangle_E = \exp\{-(t^2/2\hbar^2)(\partial E_{01}/\partial n_\phi)^2 \times \int_{-\infty}^{\infty} d\omega S_{n_\phi}(\omega)[\sin^4(\omega t/4)/(\omega t/4)^2]\} = \exp[-(\Gamma_{\varphi E}^g t)^2]$, where $\Gamma_{\varphi E}^g = (\sqrt{A_{n_\phi}\ln 2}/\hbar)|\partial E_{01}/\partial n_\phi|$ [3]. The Gaussian decay function is characteristic of the $1/f$ noise spectrum which has a singularity at low frequency. The n_ϕ dependence of $\Gamma_{\varphi E}^g$ follows $|\partial E_{01}/\partial n_\phi| = |\varepsilon|/\sqrt{\varepsilon^2 + \Delta^2}$, which is basically linear in the range of n_ϕ studied, as shown in Figs. 4(b) and 4(e).

Free-induction decay measurement also supports the interpretation. As shown in Figs. 4(c) and 4(f), the Gaussian decay rate $\Gamma_{\varphi F}^g$ also increases almost linearly with $|n_\phi - n_\phi^*|$ [15]. The asymptotic value of the ratio $\Gamma_{\varphi F}^g/\Gamma_{\varphi E}^g$ at large $|n_\phi - n_\phi^*|$ was between 4.5 and 7.5 for all the samples measured, which demonstrates that the echo procedure largely suppresses the dephasing and that the flux noise has a significant amount of low-frequency spectral weight. The ratio $\Gamma_{\varphi F}^g/\Gamma_{\varphi E}^g$ was slightly larger than expected ($\sqrt{\ln(1/\omega_{ir}t)/\ln 2} \sim 5$ [4]) for $1/f$ noise with an infrared cutoff frequency $\omega_{ir}/(2\pi) \sim 1$ Hz determined by the measurement procedure. We could imagine there exist some additional low-frequency fluctuations contributing mainly to $\Gamma_{\varphi F}^g$. An alternative scenario is an ultraviolet

cutoff which would make the ratio larger, as suggested in Ref. [4] for $1/f$ charge noise. However, such a cutoff should modify the Gaussian decay function of $\langle e^{i\varphi(t)}\rangle_E$, which we did not observe.

We evaluated the amplitude of the $1/f$ flux noise from the $|\partial E_{01}/\partial n_\phi|$ fitting of $\Gamma^g_{\varphi E}$ and obtained $\sqrt{A_{n_\phi}} = 9.3 \times 10^{-7}$ and 9.9×10^{-7} for samples A and B, respectively [19]. Three other samples also gave $(1.1 - 2.0) \times 10^{-6}$ reproducively, though the origin of the $1/f$ flux noise remains to be understood. One may suspect that the critical-current fluctuations of the SQUID junctions produce the $1/f$ flux noise via the change of the SQUID circulating current. However, the normalized $1/f$ critical-current fluctuations of the reported value $\sim(10^{-6})^2/\mathrm{Hz}$ at 1 Hz [20,21] would give at most 1% of the $\sqrt{A_{n_\phi}}$ for the mutual inductance of $\sim$20 pH between the qubit and the SQUID. It may be worth mentioning that in SQUIDs with much larger dimensions a similar amount of low-frequency flux noise has been known for a long time [22] and not yet understood either.

It is also interesting to compare the present result with a previous work on a flux qubit where the dominant dephasing was attributed to thermal fluctuations of photon numbers in the plasma mode of the readout SQUID [7]. There are a few noticeable differences in the result of Ref. [7]: (i) The echo decay was exponential; (ii) $\Gamma_{\varphi E}$ scaled with $(\partial E_{01}/\partial n_\phi)^2$ as a function of n_ϕ; (iii) the echo decay rate was smallest at $n_\phi \neq n^*_\phi$ when $I_b \neq I^*_b$. In our experiment, $\Gamma^g_{\varphi E}$ was smallest at $n_\phi = n^*_\phi$ for any I_b (data not shown). Indeed, our estimation shows that, even in the presence of the same amount of $1/f$ flux noise as in our samples, the contribution would have been concealed by the photon-number fluctuations in the sample in Ref. [7]. In the present work, on the other hand, the dephasing rate due to the photon-number fluctuations is more than an order of magnitude smaller. This is mainly because the coupling factor $|\partial^2 n^*_\phi/\partial I^2_b|$, which increases rapidly when the bias flux through the readout SQUID approaches half-integer flux quanta, is about 5 times smaller in our samples.

In conclusion, we have studied decoherence in flux qubits. We presented the qualitative difference between decay functions at different bias conditions and characterized the noises contributing to the decoherence. We demonstrated that $1/f$ flux noise constituted one of the main decoherence sources. On the other hand, the effect was suppressed at the optimal flux bias point where the energy-relaxation process turned out to be the limiting factor of the coherence in the echo decay. Reducing the energy-relaxation rate is the key issue in improving the coherence of flux qubits further.

We are grateful to O. Astafiev, P. Bertet, J. Clarke, D. Estève, S. Lloyd, Yu. Makhlin, J. Martinis, and A. Shnirman for valuable discussions.

[1] Yu. Makhlin, G. Schön, and A. Shnirman, Rev. Mod. Phys. **73**, 357 (2001).
[2] D. Vion *et al.*, Science **296**, 886 (2002).
[3] A. Cottet, Ph.D. thesis, Université Paris VI, 2002.
[4] G. Ithier *et al.*, Phys. Rev. B **72**, 134519 (2005).
[5] O. Astafiev *et al.*, Phys. Rev. Lett. **93**, 267007 (2004).
[6] T. Duty, D. Gunnarsson, K. Bladh, and P. Delsing, Phys. Rev. B **69**, 140503(R) (2004).
[7] P. Bertet *et al.*, Phys. Rev. Lett. **95**, 257002 (2005).
[8] R. W. Simmonds *et al.*, Phys. Rev. Lett. **93**, 077003 (2004); K. B. Cooper *et al.*, *ibid.* **93**, 180401 (2004); J. M. Martinis *et al.*, *ibid.* **95**, 210503 (2005).
[9] J. Claudon, A. Fay, L. P. Lévy, and O. Buisson, Phys. Rev. B **73**, 180502(R) (2006).
[10] J. E. Mooij *et al.*, Science **285**, 1036 (1999).
[11] Here we approximately decompose the flux induced by the SQUID circulating current into the sum of an I_b-dependent part Φ_{I_b} and a part depending on the flux in the SQUID loop. We define Φ_{ex} including the latter term.
[12] G. Burkard *et al.*, Phys. Rev. B **71**, 134504 (2005).
[13] I. Chiorescu, Y. Nakamura, C. J. P. M. Harmans, and J. E. Mooij, Science **299**, 1869 (2003).
[14] The qubit state can be read out even if it is operated at $n_\phi = n^*_\phi$, where the two eigenstates have zero expectation values of persistent current, since the applied current pulse adiabatically shifts the flux bias condition before reaching the switching current [13].
[15] Although FID curves at the optimal point often showed a beatinglike envelope as seen in Fig. 2(b), the curves were fitted better with a regular envelope when $|n_\phi - n^*_\phi|$ or $|I_b - I^*_b|$ is larger.
[16] $S_\lambda(\omega) \equiv \frac{1}{2\pi}\int^{\infty}_{-\infty} d\tau \langle \widehat{\delta\lambda}(0)\widehat{\delta\lambda}(\tau)\rangle e^{-i\omega\tau}$ is defined as the unsymmetralized noise spectral density.
[17] A. Shnirman, Yu. Makhlin, and G. Schön, Phys. Scr. **T102**, 147 (2002); Yu. Makhlin and A. Shnirman, Phys. Rev. Lett. **92**, 178301 (2004).
[18] To deconvolute the decay curves and obtain $\Gamma^g_{\varphi E}$, we fit the raw data $P_{\mathrm{sw}}(t)$ with $P^\infty_{\mathrm{sw}} + A\exp[-(\Gamma_1 t/2) - (\Gamma^g_{\varphi E} t)^2]$, using Γ_1 obtained from energy-relaxation measurement and P^∞_{sw}, A, and $\Gamma^g_{\varphi E}$ as free parameters in the least-square fit. Then $\langle e^{i\varphi(t)}\rangle_E$ is calculated as $[P_{\mathrm{sw}}(t) - P^\infty_{\mathrm{sw}}]/[A\exp(-\Gamma_1 t/2)]$. A similar procedure is used for FID.
[19] In the conventional expression in $1/f$ noise measurements at $f > 0$, $S_{n_\phi}(f) \equiv 2A_{n_\phi}/f$ [1/Hz].
[20] F. C. Wellstood, C. Urbina, and J. Clarke, Appl. Phys. Lett. **85**, 5296 (2004).
[21] J. Eroms *et al.*, cond-mat/0604306.
[22] F. C. Wellstood, C. Urbina, and J. Clarke, Appl. Phys. Lett. **50**, 772 (1987).